Available online at www.sciencedirect.com

ScienceDirect

Advances in Space Research 68 (2021) 2677–2694

ADVANCES IN SPACE RESEARCH (a COSPAR publication)

www.elsevier.com/locate/asr

Initial orbit determination methods for track-to-track association

Alejandro Pastor [a,b,*], Manuel Sanjurjo-Rivo [b], Diego Escobar [a]

[a] GMV, 11 Isaac Newton, 28670 Tres Cantos, Madrid, Spain
[b] Universidad Carlos III de Madrid, 30 Avenida Universidad, 28911 Leganés, Madrid, Spain

Received 8 December 2020; received in revised form 23 April 2021; accepted 20 June 2021
Available online 13 July 2021

Abstract

The detection and identification of Resident Space Objects (RSOs) from survey tracks requires robust and efficient orbit determination methods for the association of observations of the same RSO. Both Initial Orbit Determination (IOD) and Orbit Determination (OD) methods perform the orbital estimation in which the association of tracks relies. The choice of proper IOD and OD methods is essential for the whole data association, since they are in charge of providing the estimation required to evaluate the figure of merit of the association. In this paper, we review the state of the art and propose a novel method that does not require initialisation, accounts for measurement noise and provides a full estimation (i.e., state vector and covariance) from an arbitrary number of optical observations. To do so, a boundary value problem is formulated to find a pair of ranges leading to a minimum residuals of the observations. The proposed methods are compared against classical alternatives simulated in scenarios representative of the current space debris environment.

Keywords: Initial orbit determination; Orbit determination; Track-to-track association

1. Introduction

The enhancement of the sensing capabilities to observe RSOs is posing the challenge of a timely and suitable data processing, in the context of Space Situational Awareness (SSA) and Space Traffic Management (STM) (Johns et al., 1990). The increasing congestion of the orbital debris environment makes cataloguing activities more demanding year after year. For the time being, most of the catalogues contain only RSOs as small as 10 cm, reaching thousands of entries (e.g. around 20,000 in Space-Track (18th Space Control Squadron, 2020) and 5,000 in JSC Vimpel (JSC Vimpel Interstate Corporation and the Keldysh Institute of Applied Mathematics, 2020)), but they are becoming more massive thanks to initiatives such as the Space Fence System (Haimerl and Fonder, 2015). During surveillance, large areas of the sky are scanned by Space Surveillance and Tracking (SST) sensors to gather large amounts of data for both build-up and maintenance of these catalogues. The efficient and automated use of this data involves data association and estimation techniques. Otherwise, automatic processing and high sensing data usage rates cannot be completely attained (Domínguez-González et al., 2017).

Before giving a precise definition of the problem, the authors find it necessary to clarify some terms that are extensively used along this paper and whose meaning may vary from one author to another:

Observation: set of measurements taken from a single sensor at a common epoch, t, and originated from the same RSO.

Track: set of n observations taken by a single sensor usually over a short time period, originated from the

* Corresponding author.
E-mail addresses: alejandro.pastor@alumnos.uc3m.es (A. Pastor), msanjurj@ing.uc3m.es (M. Sanjurjo-Rivo), descobar@gmv.com (D. Escobar).

https://doi.org/10.1016/j.asr.2021.06.042
0273-1177/

same RSO and not enough to reliably estimate an orbit. Tracks from optical and radar surveillance sensors are usually referred to as uncorrelated optical observations (UCOs) and uncorrelated tracks (UCTs), respectively.

From an operational point of view, a single track itself is not enough to estimate an orbit with which to provide SSA and STM services because the associated uncertainty is too large (Milani et al., 2004). In fact, these are also referred to as tracklets, Short Arcs (TSAs) or Very Short Arcs (VSAs) (Tommei et al., 2007). The complete and efficient use of these sensing data is only possible by solving the track-to-track association (often called track-to-track correlation) problem, where estimation and correlation are highly coupled: to detect a new RSO it is required to estimate its orbit, but only sensing information belonging to the same RSO should be used in this estimation. This problem is known as Observation-To-Observation Association (OTOA) within the tracking community (e.g. Bar-Shalom, 1981; Blackman, 2004; Uhlmann, 2008), although here it is referred to as track-to-track association. The detection of new RSOs necessarily entails track-to-track association, since a single track is not enough to reliably initialise a new orbit in the catalogue (Hill et al., 2012; Fontdecaba i Baig et al., 2011).

Usually, prior association of the observations within a track is assumed (Hussein et al., 2015), since most sensors perform correctly this preliminary association given the short time between observations (Herzog et al., 2013; Stauch et al., 2018). In other words, we assume that the set of observations contained on a track belong to the same RSO. A preliminary step in the processing of associations of tracks is the observation compression. Observation compression consists in transforming a set of observations collected by a sensor (i.e., track) into a single observation, known as attributable (Milani et al., 2001), at the middle epoch of the observations, t_0:

$$\mathcal{A} = \left\{\hat{\boldsymbol{z}}(t_0); \hat{\dot{\boldsymbol{z}}}(t_0)\right\}$$

where hat denotes an estimated value. The benefits of observation compression are three: 1) mitigation of measurement noise effect, 2) reduction of the number of measurements and 3) estimation of measurement rates. It is a basic pre-processing technique used in data association and correlation problems (Stauch et al., 2018). This compression can be achieved by a least-squares low degree fit to the observations of the track and the rate of change of a measurement is obtained by simply deriving the interpolation polynomial. If the track is long enough, it might be even possible to extract more than one meaningful fitted observations from a single track. Most IOD methods use a limited number of observations, only two or three, while both radar and optical tracks usually contain more observations. Therefore, observation selection and compression techniques are required to maximise orbit observability during IOD.

Track-to-track association relies on IOD methods to obtain the first estimation of an orbit. During the first steps of the association process only few observations are available, and therefore an accurate orbit cannot be estimated. However, a rough estimate of the semi-major axis, eccentricity or inclination allows defining filters to reduce the complexity of the problem. For instance, if the inclination of the orbit estimated from two associations of tracks differed more than 30 degrees, then the likelihood of the hypothesis that the tracks from the two associations belong to the same object would be so low that we may want to avoid evaluating it. In fact, complexity reduction techniques allow to divert from brute-force methods. Track association is a NP-hard (Non-deterministic Polynomial-time hard) combinational optimisation problem, i.e. the computational cost increases exponentially with the number of objects. Since operational real-time track-to-track association scenarios involve a large number of tracks and objects, IOD methods for this purpose are required to be both robust and computationally efficient. Note that a failed IOD may prevent an object to be detected in data-starved environments. Moreover, IOD is followed by OD, which refines the initial solution by considering all available observations.

Multi Target Tracking (MTT) methods, traditionally applied to sensing, guidance, navigation and air traffic control, among others (Pulford, 2005), have also been used to tackle the track association problem. Joint Probabilistic Data Association (JPDA) (Stauch et al., 2018), Multiple Hypothesis Tracking (MHT) (Singh et al., 2013) and Random Finite Sets (RFS) (Jones and Vo, 2015) are very promising frameworks for the build-up and maintenance of catalogues of RSOs, although they are still under research. IOD and OD methods are key algorithms supporting and driving the estimation processes of these methodologies and deserve special attention, since they were not originally conceived for data association purposes.

Some proposed approaches to solve the track association problem use classical IOD methods (Siminski, 2016; Vananti et al., 2016), while others incorporate the so-called Statistical Initial Orbit Determination (SIOD) methods, aimed at improving the knowledge of the probability density function describing the estimation processes (Hussein et al., 2015; Stauch et al., 2018). The use of SIOD methods in operational environments is still under research and not yet completely mature. However, they can still benefit from this work, since the concepts discussed hereafter are applicable.

IOD consists in obtaining the first guess of the orbit without a priori information. A broad set of IOD methods are available in the literature for different number and types of observations (mainly optical and radar). These methods are usually limited in the sense that they require a certain number of observations containing fixed types of measurements (e.g., right ascension and declination at three observation epochs) to provide limited orbit data

(e.g., state vector at the first observation epoch). The selection of the most suitable IOD method is not an easy task because of the large number of parameters and considerations involved and the absence of a universal IOD method to apply in any situation. Besides, a suitable balance between computational effort and association performance is sought.

Classical IOD methods have not been conceived for track-to-track association, which requires certain sequential and computational cost effectiveness, given the large amount of hypotheses to be evaluated. There is a relevant trade-off in the share of the computational cost between IOD and OD, taking into account that the accuracy of the IOD solution has a direct impact on the number of iterations required by the OD to converge, assuming a batch least-squares estimation process. This is a relevant trade-off in track-to-track association given the intensive use of these methods for the evaluation of large sets of hypotheses. Thus, the goal of the IOD during track-to-track association should be to provide *an accurate enough* solution for the subsequent OD in the shortest possible time, rather than *the best* solution achievable.

The usual approach is a two-step IOD + OD methodology to obtain the estimation, required to evaluate any track association metric. This strategy might be enough for the association of radar tracks since they contain more information (range and/or Doppler measurements) than optical ones, although the error associated to radar angular measurements is usually two orders of magnitude greater than the optical counterpart (Schildknecht, 2007; Rodriguez Fernandez et al., 2018). This makes the association of optical tracks more challenging than that of radar tracks and it is precisely in this case when the traditional IOD + OD estimation chain might not be the best option and thus alternative strategies are required.

In this paper, we propose a novel joint methodology aimed at evaluating associations of optical tracks. It is able to provide an estimate without initialisation for an arbitrary number of observations. The main difference with respect to classical methods, such as Gooding's method (Gooding, 1993) and double r-iteration method Escobal (1965), is that the IOD problem is formulated as a batch least-squares orbit determination. This allows to include three or more observations, to take into account measurement noise and to obtain a full estimation of the orbit (i.e., state and covariance), which are important features to address the track association problem. Besides, the proposed methodology enables to move from a two-step IOD + OD methodology to a single one. We compare its performance against classical alternatives on an operational-like simulated scenario. Apart from presenting the new methodology, we discuss additional aspects of track-to-track association, sometimes skipped in the literature, that play an important role in an operational scenario. The goal of this paper is to present IOD methods that can be used during the massive and operational track association problems. Accordingly, the focus is on the estimation problem, rather than the correlation one. The proposed methods have been already used for track-to-track association with radar (Pastor et al., 2018) and optical (Pastor et al., 2019) observations.

In Section 2, we review the state of the art IOD + OD estimation processes, emphasising on the radar survey problem, for which existing methods are generally enough. In Section 3, we introduce novel methods for the particular optical survey problem. In Section 4, we provide and discuss results to evaluate the performance of the proposed methods and compare them against classical alternatives. Finally, in Section 5, we summarise and discuss the conclusions of this paper.

2. State of the art methods

In this section, the IOD and OD state of the art is presented, emphasising on the most relevant aspects for the track association problem. Then the role of these methods in the traditional two-step IOD + OD estimation chain is discussed, highlighting the need of a different approach in the optical survey association case.

Before continuing with the state of the art IOD methods, a brief background on orbit geometry, depicted in Fig. 1, is presented. Firstly, the position vector of an object, $\boldsymbol{r}$, is determined by its topocentric right ascension, α, topocentric declination, δ, and range, ρ, since:

$$\boldsymbol{r} = \boldsymbol{R} + \rho \boldsymbol{L} \tag{1}$$

where $\boldsymbol{R}$ is the position vector of the sensor station (or satellite in the case of space-based sensors) and $\boldsymbol{L}$ is the line of sight vector (also known as pointing vector), which is a function of the right ascension and declination:

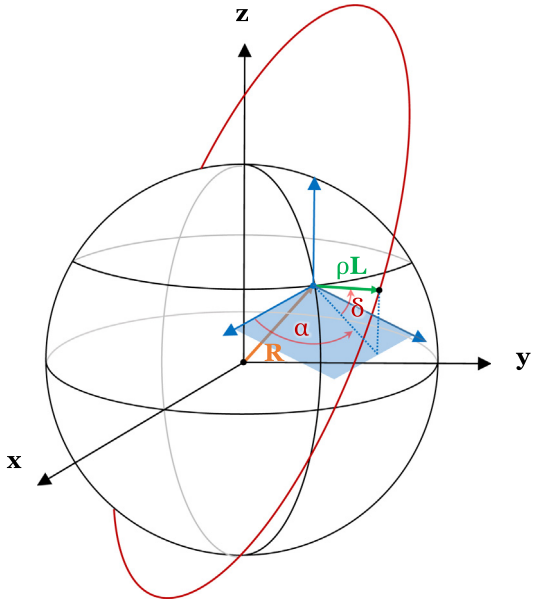

Fig. 1. Sketch of a typical observation geometry.

$$\boldsymbol{L}(\alpha,\delta)=\begin{Bmatrix}\cos\alpha\cos\delta\\ \sin\alpha\cos\delta\\ \sin\delta\end{Bmatrix} \tag{2}$$

Solving the second order equation for the range obtained by the dot product of Eq. (1) with itself, the so-called range equation is obtained:

$$\rho=\frac{-c+\sqrt{c^2-4\left(R^2+r^2\right)}}{2} \tag{3}$$

being $c=2\boldsymbol{R}\cdot\boldsymbol{L}$.

Secondly, the velocity vector of an object, $\boldsymbol{v}$, is obtained by differentiating Eq. (1) with respect to time:

$$\boldsymbol{v}=\dot{\boldsymbol{R}}+\dot{\rho}\boldsymbol{L}+\rho\dot{\boldsymbol{L}} \tag{4}$$

where $\dot{\boldsymbol{R}}$ is the sensor station velocity vector, $\dot{\rho}$ is the range-rate and $\dot{\boldsymbol{L}}$ is the rate of change of the line of sight vector, given by:

$$\dot{\boldsymbol{L}}\left(\alpha,\delta,\dot{\alpha},\dot{\delta}\right)=\begin{Bmatrix}-\dot{\alpha}\sin\alpha\cos\delta-\dot{\delta}\cos\alpha\sin\delta\\ \dot{\alpha}\cos\alpha\cos\delta-\dot{\delta}\sin\alpha\sin\delta\\ \dot{\delta}\cos\delta\end{Bmatrix} \tag{5}$$

2.1. Initial Orbit Determination methods

Traditionally, the IOD problem has been tackled as a deterministic problem and solved using algebraic approaches. Laplace in 1780 (Laplace, 1780) and Gauss in 1801 (Gauss, 1809) conceived the first methods to estimate the position vector of an object given three pairs of angular measurements (Escobal, 1965). Since then, many more methods have been developed using different measurement types: angles only (Gooding, 1993), position vectors (Jordan, 1964), angles and range-rate (Yanez et al., 2017), angles only without time information (Zeinalov, 1973)...); and a wide variety of approaches: energy variance (Morton and Taff, 1986), admissible regions (Milani et al., 2004), keplerian integrals (Gronchi et al., 2016), among others. Moreover, stochastic approaches have been proposed (DeMars and Jah, 2013; Armellin and Lizia, 2016), enabling them to provide uncertainty-related information (Weisman and Jah, 2014; Armellin et al., 2016).

One of the IOD methods for optical observations preferred in operational environments is Gooding's method (Gooding, 1993). It was conceived as an alternative to the traditional methods of Laplace and Gauss, free of their inherent limitations, but requiring the same number of angular observations or attributables: three. The idea beneath this method is to use a universal solution of the Lambert's problem developed by Gooding (Gooding, 1990) to perform a higher-order Newton correction of the two unknown ranges (double r-iteration method in Escobal (1965)). Although, it is capable of performing IOD on three observations from a single track, this is not generally the best case of application due to the limited observability given the typically low track time span if compared to the orbital period (Fadrique et al., 2011). Therefore, two tracks or preferably three are usually required, and thus a method to select a solution is generally needed, since it may provide more than one solution. Most recent methods include the consideration of uncertainty in the measurements, as opposed to classical methods. In general, the IOD problem can be tackled as an initial or boundary value problem. Regarding the former, an initial state consisting in available measurements (angles) is extended with certain hypotheses (range and range-rate) and propagated to a final epoch, at which predicted and actual measurements are compared. On the other hand, the latter ones extend two states with certain hypotheses (ranges) to build a Lambert's problem. The hypotheses hyperplane can be sampled by means of admissible regions (DeMars et al., 2012; Fujimoto et al., 2013; Gronchi et al., 2016) and the solution is found after solving a minimisation problem (Siminski et al., 2014).

Regarding IOD methods for radar observations, Gibbs method has been a typical choice. It is a method that allows to obtain the orbit by using a pair of angles and the range at three epochs, i.e. three position vectors or three radar attributables. The complete algorithm and details can be found in Vallado (1997). The method is geometric, based on vector analysis, and therefore vector spacing is of major importance: the position vectors have to be spaced enough so as to minimise numerical instabilities. Herrick-Gibbs method is a variation of Gibbs method focused on providing reliable results when vector spacing is very small, i.e. the observation are obtained in a short time (compared to the orbital period). This is the typical set of observations contained on a single track provided by a sensor. Finally, Goddard Trajectory Determination System (GTDS) Range and Angles method iteratively estimates the position and velocity by fitting the f and g functions of the two-body motion with more than two radar observations (i.e. range and angles) (Long et al., 1989). If applied to a single track, this method tends to provide better estimations than solving the Lambert's problem (Jordan, 1964), mainly because it uses all the available observations and not just two (Vananti et al., 2016). Since all the observations from the track are considered, this method is analogous to a two-body motion least-squares OD.

Moreover, some of the aforementioned methods provide several solutions to the IOD problem, being the selection of the best, or at least pruning of spurious ones, required for a fully automated track-to-track association data processing scheme. Although many solutions may be found, only one may correspond to the true orbit and thus, the rest should be pruned as they represent spurious solutions. A priori information, i.e. knowledge of certain orbit parameter, can be used to select the best candidate solution, e.g. the solution with closest semi-major axis to Geostationary Earth Orbit (GEO) can be selected. Heuristic approaches, using catalogued space debris population statistics, assigning to each solution certain probability (Olmedo et al.,

2008), is an alternative when lacking a priori information. Finally, selecting the solution with lowest residuals with respect to all available observations (i.e. before observation compression) is a very suitable criteria and does not require a priori nor external information. Besides, it allows to use raw observation data to perform the selection, rather than a subset of attributables (used during IOD).

Stating that an IOD method requires n observations does not necessarily refers to n observations from a single track, but n observations obtained by compressing N separated tracks (each of which may have different number of observations), i.e. N attributables. This distinction is relevant in terms of observability.

2.2. Orbit Determination methods

OD performs a refinement of the IOD solution by considering larger sets of data. The benefits of performing OD estimation after IOD are twofold: 1) use the entire dataset of observations in a statistical way and 2) enable the use of more complex dynamical models. On the basis of the first aspect, the statistical approach of OD, as opposed to the usually deterministic IOD, provides uncertainty characterisation (covariance under a Gaussian process assumption, Poore et al. (2016)) and meaningful residuals information, both essential ingredients to evaluate figures of merit in the track-to-track association problem (Hill et al., 2008; Stauch et al., 2018; Hussein et al., 2015). Regarding the second aspect, unlike most IOD methods, the dynamical model driving the estimation is not limited to the two-body motion. This is very relevant in particular cases, such as High Area-to-Mass Ratio (HAMR) (Schildknecht, 2005) or very low Low Earth Orbit (LEO) (Bennett et al., 2012) RSOs.

Both batch (Pirovano et al., 2020, 2017,) and sequential (Sha et al., 2017; Stauch et al., 2018; Aristoff et al., 2013; Jones and Vo, 2015) estimators have been used in track-to-track association. Batch estimation provides an easier interpretation of the results: performing the estimation in batches allows to directly obtain the contribution of each observation to the solution. As a matter of fact, when performing OD on N tracks, the contribution of the i^{th} track to the information matrix is clear, as well as the covariance and residuals contributions. On the contrary, sequential estimation itself, requires additional smoothing techniques to achieve similar results as batch estimation (Stauch et al., 2018). Besides, sequential estimations using large sets of observation(s) may result in too optimistic (close to zero) covariance matrices, leading to insensitivity to additional observations if process noise is not properly accounted for (Tapley et al., 2004).

A common drawback of both estimators is the underlying linearisation of the problem around a reference state that is usually initialised with the IOD solution. If the latter is far from the true state then the estimation procedure may not converge, or even worse, converge to a local minimum, due to the intrinsic non-linearity of the problem. In the case of sequential estimators, this can be minimised by updating the reference trajectory after adding each observation, the main concept behind Extended Kalman Filter (EKF) (Bar-Shalom et al., 2001; Tapley et al., 2004). Regarding batch estimators, the Levenberg–Marquardt algorithm (Marquardt, 1963) improves the radius of convergence with respect to the classical Gauss–Newton solver (Warner and Lemm, 2016). Although the use of the Levenberg–Marquardt algorithm increases the computational cost, it is a very suitable feature for track-to-track association, where limited observability and ill-conditioned problems are commonplace. For instance, re-entry orbit estimation, where an orbit must be determined from a small set of available measurements without any additional information (catalogued orbit may lack sufficient accuracy) under highly non-linear dynamics (Alarcón et al., 2005).

Finally, the dynamical model used for orbit determination must be selected according to the 1) computational cost (given the large number of hypotheses to go through the estimation chain), 2) accuracy required (e.g., the score derived from the estimation should allow to distinguish between RSOs) and 3) available information (e.g., drag coefficient cannot be reliably estimated from a single track). Two-body motion dynamics provide the lowest computational cost at the expense of a decrease in accuracy. On the other hand, high-fidelity numerical propagators, able to consider non-spherical Earth gravity, third bodies, atmospheric forces and solar radiation pressure, among others, allow to attain a unrivalled accuracy, although the computational cost associated is rather high. Finally, semi-analytical and analytical dynamical models based on mean elements: Draper Semi-analytical Satellite Theory (DSST) (Cefola, 2012), Eckstein-Hechler (Eckstein and Hechler, 1970), Simplified General Perturbations (SGP) (Vallado et al., 2006) or Brouwer-Lyddane (Galbreath, 1970), among others; are very suitable compromise solutions thanks to their balance between accuracy and computation effort.

2.3. IOD + OD estimation chain

Track-to-track association is usually performed in an incremental way in the sense that associations of N tracks are generated from associations of $N-1$ tracks, e.g. two single tracks are associated to give rise to a pair, two pairs with a common track are associated to give rise to a triplet, two triplets with common tracks are associated to give rise to a quadruplet and so on. In such a way, an association of N tracks has at least two parent associations of $N-1$ tracks. Once the associations (hypotheses in the MHT framework) are generated, they are usually evaluated by means of an IOD + OD estimation chain, depicted in Fig. 2. Here we see the IOD and OD processes proposed for the scoring of a hypothesis. MHT algorithms, such as gating (pruning of clearly wrong hypotheses) or promotion (final identification of a new detection) are based on the outcome of this scoring procedure (evaluation of certain

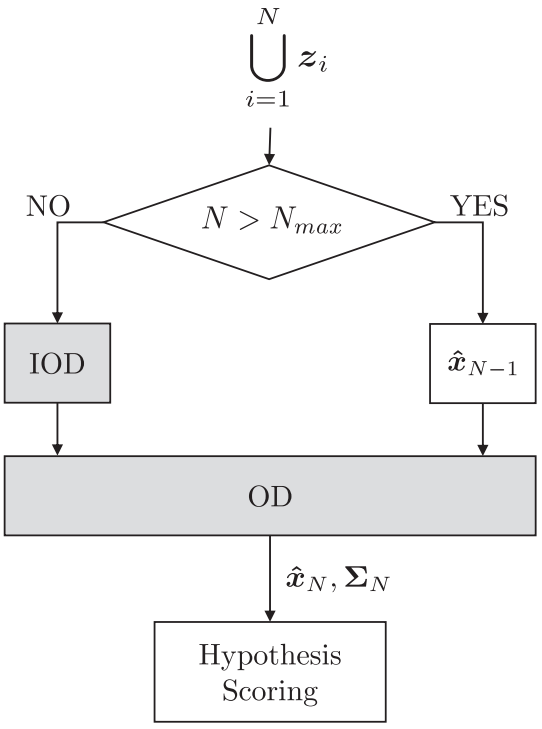

Fig. 2. Sketch of the state of the art IOD + OD association estimation chain.

figure of merit or likelihood), and therefore on the outcome of the estimation chain. There are two limiting values of N:

- Lack of information ($N < N_{min}$): there is not enough data to reliably obtain an IOD solution. The hypothesis cannot be processed until more tracks are associated.
- Enough a priori information ($N > N_{max}$): the previous estimations coming from the parent associations of $N-1$ tracks are close enough to be used as initial solution during OD and thus IOD is not required.

2.3.1. Radar survey problem

The information contained in a single radar track, although maybe not enough to reliably estimate an orbit, usually allows to perform OD using simple IOD methods for the generation of the initial solution. In this situation, $N_{min} = 1$, and therefore no brute-force is required for the generation of associations of two tracks, since a first (albeit rough) estimation of the orbit is available.

Generally, tracks from radars contain more observations than optical sensors due to their larger field of view. Usually, many observations are available in a relatively small time span, so it makes sense to perform the observation compression. Since the latter provides also the rates of the measurements, it is then possible to compute a state vector and finally to average all the state vectors (using equinoctial elements (Broucke and Cefola, 1972) for instance) to obtain the solution. This IOD method, which we refer to as *State Vector Fitting*, is summarised in Algorithm 1. A further improvement is to use the position vectors obtained from the observation compression but to estimate a new velocity vector by solving a Lambert's problem with Izzo's solver (Izzo, 2014). Moreover, the solution provided by the observation compression can be used to fix the number of revolutions and the motion type (prograde or retrograde) thus solving a restricted Lambert's problem (with a lower number of solutions).

Algorithm 1. State Vector Fitting method

Require: $\{\alpha, \delta, \rho\}_i^j$ for $i = 1, \ldots, n_j$ and $j = 1, \ldots, N$ with $N \geqslant 2$ tracks
for $j = 1, \ldots, N$ **do** ▷ Loop on tracks
  Fit n_j observations:

$$\{\alpha, \delta, \rho\}_{i=1,\ldots,n_j}^j \rightarrow \left\{\hat{\alpha}, \hat{\delta}, \hat{\rho}; \hat{\dot{\alpha}}, \hat{\dot{\delta}}, \hat{\dot{\rho}}, \right\}^j$$

  Compute $\hat{\boldsymbol{r}}_j$ (Eq. (1))
  if *Lambert mode* **then**
    for $k = 1, \ldots, j-1$ **do** ▷ Loop on previous tracks
      Compute n_{rev} between $\boldsymbol{r}_j$ and $\boldsymbol{r}_k$
      Compute motion type: $\eta \in \{+1, -1\}$
      Solve restricted Lambert's problem:

$$\{\hat{\boldsymbol{v}}^j, \hat{\boldsymbol{v}}^k\} = \mathcal{L}\left(\hat{\alpha}^j, \hat{\delta}^j, \hat{\rho}^j, \hat{\alpha}^k, \hat{\delta}^k, \hat{\rho}^k, \Delta t^{jk}; n_{rev}^{jk}, \eta^{jk}\right)$$

    end for
  else
    Compute $\hat{\boldsymbol{v}}^j$ (Eq. (4))
  end if
  Transform into equinoctial elements: $\{\hat{\boldsymbol{r}}, \hat{\boldsymbol{v}}\}^j \rightarrow \hat{\alpha}^j$
end for
Average solutions: $\{\hat{\alpha}\}^{j=1,\ldots,N} \rightarrow \langle\hat{\alpha}\rangle$
Transform equinoctial elements to state vector: $\langle\hat{\boldsymbol{r}}\rangle \rightarrow \langle\hat{\alpha}\rangle$

2.3.2. Optical survey problem

On the contrary, the information contained on a single optical track, does not allow to perform IOD, i.e.: $N_{min} > 1$, meaning that the generation of associations of $N < N_{min}$ optical tracks entails a significant level of brute-force.

Accordingly, our proposal in this case is to move from a two-step IOD + OD methodology to a single one, presented in Section 3, that 1) does not require any initial guess nor a priori information, 2) provides metrics for the track-to-track association problem, and 3) can be used with an arbitrary number of tracks and observations.

3. Novel methods

We propose a novel method to replace the two-step IOD + OD estimation chain that arises during the evaluation of hypotheses during optical track association: double r-iteration method. For completeness, before introducing the method, we present the Circular method, not proposed here to be used standalone but as a part of double r-iteration Lambert.

3.1. Circular method

As shown in Fig. 3, where both the histogram and Cummulative Distribution Function (CDF) are presented, most of the objects present in the Satellite Catalogue (SATCAT) from Space-Track (Kelso, 2020) are following nearly circular orbits. In fact, 92% of them are describing orbits with $e < 0.1$ and 72.4% with $e < 0.01$. That is why many IOD methods assume circular orbits, thus simplifying the problem geometry and dynamics.

The so-called circular method solves the problem of finding the radius, r leading to a time of flight, Δt, equal to the observation time span, given two optical observations. Therefore, the problem of estimating the orbital radius is reduced to solving the following non-linear equation:

$$f(r) = \Delta t - \mu^{-1/2} r^{3/2} \Delta v(r) \tag{6}$$

where Δv is the difference between true anomalies:

$$\Delta v = \arccos\left(\frac{\boldsymbol{r}_1 \cdot \boldsymbol{r}_2}{\|\boldsymbol{r}_1\|\|\boldsymbol{r}_2\|}\right) \tag{7}$$

Once r is found, the range is determined by Eq. (3) and thus the position vector by Eq. (1). Finally, the corresponding velocity can be obtained at any of the two epochs since its direction is normal to the position, lays in the orbital plane and its magnitude is the well-known velocity of a circular orbit, i.e.:

$$\boldsymbol{v}_i = \frac{1}{\sqrt{r}} \frac{(\boldsymbol{r}_1 \wedge \boldsymbol{r}_2) \wedge \boldsymbol{r}_i}{\|(\boldsymbol{r}_1 \wedge \boldsymbol{r}_2) \wedge \boldsymbol{r}_i\|} \tag{8}$$

Nevertheless, it is important to point out three additional considerations:

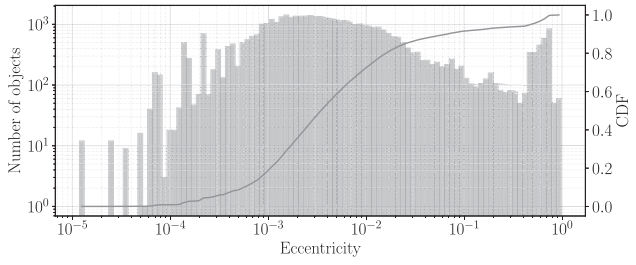

Fig. 3. Eccentricity distribution of RSOs from SATCAT as of 30 November 2020.

- *Detection of angles higher than* π: since the arccos function is not able to detect angles higher than π then the correct Δv value is $2\pi - \Delta v'$ being $\Delta v'$ the value given by Eq. (7) if the z-component of the dot product $\boldsymbol{r}_1 \cdot \boldsymbol{r}_2$ is negative.
- *Retrograde orbit*: the correction to detect angles higher than π discussed before has to be applied when the dot product $\boldsymbol{r}_1 \cdot \boldsymbol{r}_2$ is positive, since the sense of the motion is opposite. Besides, if the z-component of the cross product $\boldsymbol{r}_1 \wedge \boldsymbol{r}_2$ is negative/positive for the direct/retrograde orbit case then the sign of velocity vector in Eq. (8) has to be changed.
- *Multi-revolution*: if one or more revolutions have been completed between the first and second observations then Δv value has to be increased 2π times the number of completed revolutions, which is $n_{rev} = \text{floor}\{\mu^{1/2}\Delta t/(2\pi r^{3/2})\}$, in Eq. (7).

Eq. (6) may have more than one solution depending on the number of completed revolutions, a priori unknown. In fact, for GEO objects it is very common to obtain many solutions ranging from LEO (many completed revolutions) to GEO (few revolutions) when the object has completed at least one revolution between the two observation epochs. However, at most one of them corresponds to the orbit, being the remaining spurious solutions.

The method can be generalised to n observations, $\{1, 2, 3, \ldots, n\}$ (with $n > 2$) by estimating the orbital radii for all the $\binom{n}{2}$ measurements pairs combinations. Then, spurious solutions are selected by analysing the estimated radius differences.

The method is summarized in Algorithm 2. Note that the n observations required may come from a single track, in which case we recommend taking $n = 2$ to cover the whole arc (maximum spacing), or from n tracks (obtained via observation compression). Besides, solution selection may be necessary if more than one solution is found.

Algorithm 2. Circular method

Require: $\{\alpha, \delta\}_i$ for $i = 1, \ldots, n$ with $n \geqslant 2$
for $\{i, j\} \in \binom{n}{2}$ **do** ▷ Loop on pairs of observations
  Compute $\Delta v_{i,j}$ (Eq. (7))
  Solve Eq. (6) for $r_{i,j}$ (multiple solutions)
  for $k = 1, \ldots, n_{i,j}$ **do** ▷ Loop on solutions
    Compute $\rho^k_{i,j}$ (Eq. (3)) with $r^k_{i,j}$
    Compute $\boldsymbol{r}^k_{i,j}$ (Eq. (1)) with $r^k_{i,j}$
    Compute $\boldsymbol{v}^k_{i,j}$ (Eq. (8)) with $r^k_{i,j}$
  end for
end for
Find combinations of n solutions from pairs of $\{i, j\} \in \binom{n}{2}$
Average each combination of solutions

3.2. Double r-iteration Lambert method

Double r-iteration Lambert method, proposed as an alternative to Gooding method, is an iterative process in which two missing ranges at two separate dates are estimated in order to match additional measurements. It requires $n \geqslant 3$ observations and consists in finding two ranges with which the solution of the Lambert's problem leads to minimum residuals of the remaining $n-2$ observations. Measurements noise, in addition to the intrinsic high non-linearity of the problem, do not allow to cancel out the residuals, rendering residuals minimisation the only viable option.

Therefore, the following minimisation problem arises:

$$\begin{aligned} \min_{\hat{r}_1,\hat{r}_n} \quad & \mathcal{J} = \sum_{i=2}^{n-1}\left[\left(\frac{\hat{\alpha}_i-\alpha_i}{\sigma_\alpha}\right)^2 + \left(\frac{\hat{\delta}_i-\delta_i}{\sigma_\delta}\right)^2\right] \\ \text{s.t.} \quad & \hat{\mathbf{v}}_1, \hat{\mathbf{v}}_2 = \mathcal{L}(\alpha_1, \delta_1, \alpha_2, \delta_2, \Delta t; \hat{\rho}_1, \hat{\rho}_2,) \\ & \hat{\mathbf{r}}_i, \hat{\mathbf{v}}_i = \mathcal{F}(\hat{\mathbf{r}}_1, \hat{\mathbf{v}}_1, t_i - t_1) \qquad \forall i = 2, \ldots, n-1 \\ & \hat{\alpha}_i, \hat{\delta}_i = \mathcal{H}(\hat{\mathbf{r}}_i, \hat{\mathbf{v}}_i) \qquad \forall i = 2, \ldots, n-1 \end{aligned} \tag{9}$$

where the hat denotes estimated values, $\Delta\alpha$ and $\Delta\delta$ are the right ascension and declination residuals, σ_α and σ_δ are the right ascension and declination weights (a priori sigma), $\mathcal{L}$ represents the Lambert problem (solved with Izzo's method, Izzo (2014)), $\mathcal{F}$ the two-body motion propagator and $\mathcal{H}$ the measurement model. The objective function, $\mathcal{J}$, is proportional to the Weighted Root Mean Square (WRMS).

To avoid discontinuities in the angular residuals, Δz, i.e.: difference between actual and predicted measurements, it is advisable to use the following expression:

$$\Delta z_i = \text{atan2}\left[\frac{\sin(z_i - \hat{z}_i)}{\cos(z_i - \hat{z}_i)}\right] \tag{10}$$

A global derivative-free optimisation method could be used to explore the solution on a $\{\hat{r}_1, \hat{r}_2\}$ domain, using the admissible regions theory (Milani et al., 2004). The non-linearity of $\mathcal{J}$, illustrated in Fig. 4, would force this domain to be carefully sampled. Instead, an iterative gradient descent on the linearised problem similar to a batch least-squares orbit determination (Montenbruck and Gill, 2000) using the circular solution as initial guess is proposed:

$$[\boldsymbol{H}_{r_1}\boldsymbol{H}_{r_n}]^T \begin{bmatrix} \boldsymbol{W}_\alpha & \boldsymbol{0} \\ \boldsymbol{0} & \boldsymbol{W}_\delta \end{bmatrix} [\boldsymbol{H}_{r_1}\boldsymbol{H}_{r_n}] \begin{pmatrix} \Delta r_1 \\ \Delta r_n \end{pmatrix} = [\boldsymbol{H}_{r_1}\boldsymbol{H}_{r_n}]^T \begin{pmatrix} \hat{\alpha} - \alpha \\ \hat{\delta} - \delta \end{pmatrix} \tag{11}$$

where $\boldsymbol{H}_{r_i}$ is the Jacobian, i.e. the partials of the measurements, α and δ, with respect to r_i (can be computed analytically, Springer (2009)), $\boldsymbol{W}_z$ the weighting matrix of the measurement z and Δr_i the correction to r_i leading to the minimisation of the cost function:

$$\boldsymbol{H}_{r_i} = \begin{bmatrix} \partial\alpha/\partial r_i \\ \partial\delta/\partial r_i \end{bmatrix} \tag{12}$$

$$\boldsymbol{W}_z = diag\left(\sigma_z^{-2}, \ldots, \sigma_z^{-2}\right) \tag{13}$$

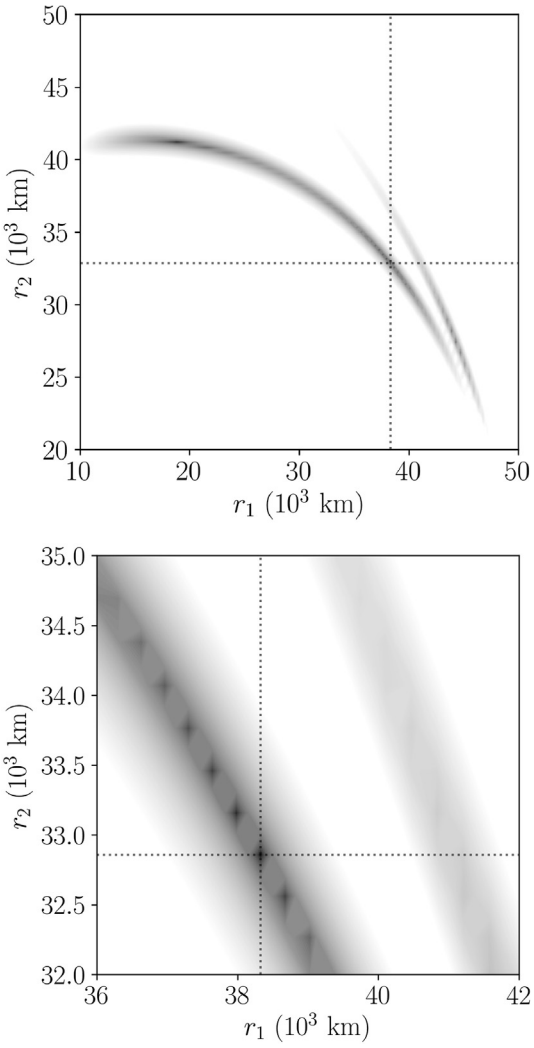

Fig. 4. Distribution of objective function of Double r-iteration Lambert method in a simulated IOD problem of a GTO RSO ($a = 24,460km, e = 0.71$) and 3 observations ($\Delta t_{12} \sim 7h, \Delta t_{23} \sim 5h$). The dotted lines represent the true values of the orbital radii.

The main difference of the proposed method, summarised in Algorithm 3, with respect to a regular OD process with two-body motion dynamics, in which position and velocity are estimated, is the number of estimated parameters. The complete (position and velocity) problem is frequently ill-conditioned (nearly singular) if only a few optical observations from a single sensor are available. On the contrary, in the proposed method a minimal set of parameters (two ranges) is estimated, thus improving the observability of the solution (Tapley et al., 2004). The same consideration as Gooding method related to the applicability to observations from a single and multiple tracks holds, except that the proposed method is able to use $n \geqslant 3$ observations in both cases. Moreover, it does not require any initial guess nor any a priori solution, and in principle, is suitable for any type of orbit, thanks to the gradient descent approach that makes initial circular

solutions converge even to highly eccentric orbits. Note that although the angular rates are not explicitly used, the dynamics of the angular measurements is included by considering every available observation. If compared to double r-iteration method (Escobal, 1965), the proposed method does not assume that the angular measurement are fixed (measurement noise is considered), is not limited to three observations and the outcome is not a single-point estimate for the ranges but a full estimation (mean and covariance). Besides, Escobal's method requires a cumbersome initialisation and iterative process (Vallado, 1997), while the proposed method can be formulated as an OD process.

Algorithm 3. Double r-iteration Lambert method

Require: $\{\alpha, \delta\}_i$ for $i = 1, \ldots, n$ with $n \geqslant 3$
1: Solve the circular problem between observation 1 and $n : \hat{r}_1, \hat{r}_n$ (Algorithm 2).
2: **for** $k = 1, \ldots, k_{max}$ **do** ▷ Iterative process
3: Compute $\hat{\rho}_1$ and $\hat{\rho}_n$ (Eq. (3)).
4: Solve Lambert's problem:

$$\hat{\boldsymbol{v}}_1, \hat{\boldsymbol{v}}_n = \mathcal{L}(\alpha_1, \delta_1, \alpha_n, \delta_n, \Delta t; \hat{\rho}_1, \hat{\rho}_n,)$$

5: **for** $i = 2, \ldots, n-1$ **do** ▷ Loop on additional obs.
6: Propagate solution: $\{\hat{\boldsymbol{r}}, \hat{\boldsymbol{v}}\}_i = \mathcal{F}(\hat{\boldsymbol{r}}_1, \hat{\boldsymbol{v}}_1, t_i - t_1)$
7: Compute measurements: $\left\{\hat{\alpha}, \hat{\delta}\right\}_i = \mathcal{H}(\hat{\boldsymbol{r}}_i, \hat{\boldsymbol{v}}_i)$
8: Compute angular residuals $\{\Delta\alpha, \Delta\delta\}^i$ (Eq. (10))
9: Compute Jacobian (Eq. (12))
10: **end for**
11: Solve Eq. (11)
12: Apply corrections: $\hat{r}_1 \leftarrow \hat{r}_1 + \Delta r_n, \hat{r}_n \leftarrow \hat{r}_n + \Delta r_n$
13: Evaluate objective function $\mathcal{J}^k$ (Eq. (9))
14: Exit if $\left\|\mathcal{J}^k - \mathcal{J}^{k-1}\right\| < \epsilon$
15: **end for**

4. Results

Two simulated scenarios are set up to assess the performance of the novel methods presented in Section 2 and Section 3, and to compare them against classical approaches: one for optical observations and another one for radar observations. Unlike usual analyses that evaluate the performance of the IOD methods for a limited set of representative cases (few objects and combinations of tracks), we have focused on studying the performance on a scenario containing a large set of tracks, aimed at determining the robustness and flexibility of the different methods. Both scenarios consist in a simulated population of RSOs representative of the current space debris environment, propagated with a high-fidelity propagator (16x16 Earth gravitational field, Moon and Sun third body perturbations, cannonball model for the Solar Radiation Pressure (SRP) and MSISE90 atmospheric density model) to avoid the matching of the dynamical model between the true and estimated states. From all the tracks of each RSO that fulfil the visibility conditions, we decided to select four tracks with a time separation representative of a track-to-track association problem. Then, we study all the IOD problems resulting from the association of i tracks, i.e.: all the $\binom{4}{i}$ combinations of i tracks: four combinations of a single track ($\{1\}, \{2\}, \{3\}, \{4\}$), six combinations of two tracks ($\{1,2\}, \{1,3\}, \{1,4\}, \{2,3\}, \{2,4\}, \{3,4\}$), four combinations of three tracks ($\{1,2,3\}, \{1,2,4\}, \{1,3,4\}, \{2,3,4\}$) and one combination of four tracks: $\{1,2,3,4\}$. To evaluate the suitability and robustness of each method in providing a solution, we consider that a method has succeeded in solving an IOD problem if it provides a solution that fulfils $\Delta a = \|a - \hat{a}\| < 10^3\, km$ (optical tracks are normally obtained in GEO). Note that the number of successes is a rough indicator of the goodness of certain method in solving a set of IOD problems, since it does not account for the accuracy of the solution. For the particular case of multi-solution methods, the one closest to the true orbit in terms of orbital parameters is selected, in order to compare the best achievable solution for each method.

Apart from the analysis of the robustness of the method, a performance assessment is carried out focused on the orbit estimation error and computational cost. For characterising the former, we opted for the orbit error defined in Mortari et al. (2006):

$$\Delta(d, \delta) = (1 + d)e^{i\delta}, \tag{14}$$

where the shape error, d, and the attitude error, δ, are given by:

$$\begin{aligned} d^2 &= a^2(2 - e^2) + \hat{a}^2(2 - \hat{e}^2) - 2a\hat{a}\sqrt{(1 - e^2)(1 - e^2)}, \\ \cos\delta &= \tfrac{1}{2}\left[tr\left(\boldsymbol{A}\hat{\boldsymbol{A}}^T\right) - 1\right], \end{aligned} \tag{15}$$

being $\boldsymbol{A} \in \mathcal{R}^{3x3}$ the orientation matrix, whose columns are the directions of the position, velocity and angular momentum vectors. This error definition allows to describe the difference between two orbits in terms of only two independent and physically meaningful quantities. The first, shape error, represents the planar position error, i.e. difference between the semi-major and semi-minor axes. The second, attitude error, represents the orientation error. Additionally, semi-major axis and eccentricity errors are also included in the analysis, for the sake of comparison with other works, as their use is more extended.

Regarding the computational cost, we evaluate the computational time, for comparison purposes only, that each IOD method takes to compute the final solution on an Intel Xeon Gold 6142 2.60 GHz CPU.

4.1. Optical observations

The simulated optical scenario consists of 514 RSOs and an optical survey sensor network consisting of four telescopes (located at Canary Islands, French Polynesia, New Caledonia and Réunion Island) receiving 2,056 tracks along one week. The semi-major axis, eccentricity and inclination of this population of RSOs are shown in Fig. 5, where the histogram and CDF are presented. The SRP coefficient has been set to 1.1 for every object and the area-to-mass ratio distribution of the RSOs is presented in Fig. 6. For each RSO, four tracks are generated including zero-mean Gaussian noise of 1 arcsec sigma, typical values used in similar analyses (Sabol et al., 2012; Siminski et al., 2014). The duration of these tracks, shown in Fig. 7 (left), has three typical values, in order of decreasing frequency: 15 s, 5.75 min and 2.92 min. The separation between each of the four tracks ranges from 6 s up to 2 min

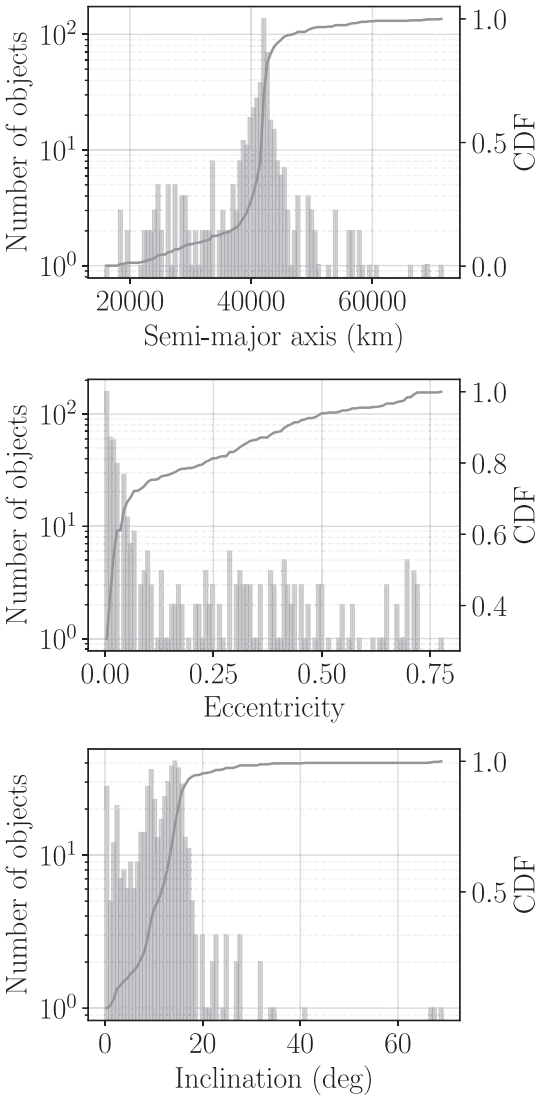

Fig. 5. Semi-major axis (top), eccentricity (center) and inclination (bottom) distribution of the population of RSOs in the optical scenario.

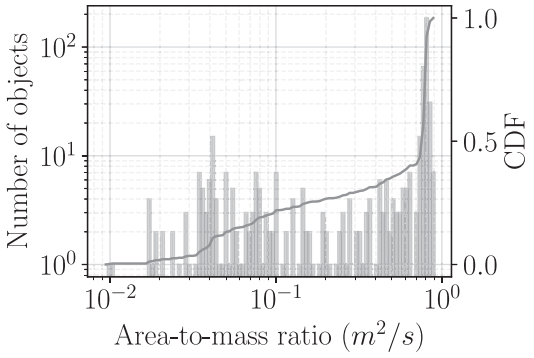

Fig. 6. Area-to-mass ratio distribution of the population of RSOs in the optical scenario.

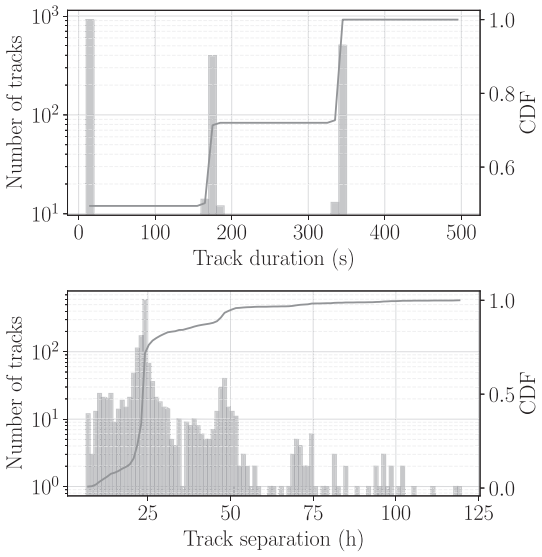

Fig. 7. Track duration (top) and separation (bottom) distributions in the optical scenario.

with peaks on multiples of 24 h, as reflected in Fig. 7 (right). The observation rate is of 0.2 s^{-1} (i.e. one observation every 5 s), similar to values used in track-to-track analyses (Vananti et al., 2017). For the optical observations case, we focus on assessing the performance of the proposed method, Double R-Iteration Lambert, and comparing against the classical alternative, Gooding's method.

Double r-iteration Lambert is applied as explained in Section 3.2, using every available observation in the tracks. Regarding Gooding's method, since it can only be applied to three observations, we compute three attributables from the available tracks. To obtain m attributables from a track, m groups of observations are set so that each group contains observations within $t_0 + (i-1)\Delta t/m$ and $t_0 + i\Delta t/m$ for $i = 1, m$, where Δt represents the track duration. In the cases of two tracks, two attributables are computed from the longest track and one from the shortest track.

The number of successes and success rate (number of successes over the corresponding total number of IOD

Table 1
Number of successes and success rate in the optical scenario.

	Number of tracks	Gooding						Double r-iteration Izzo					
		all		e<0.1		e>0.1		all		e<0.1		e>0.1	
All comb.	1	50	2.4%	15	1.0%	35	6.5%	67	3.3%	42	2.8%	25	4.6%
	2	1,023	33.2%	674	29.6%	349	43.1%	2,712	87.9%	2,251	99.0%	461	56.9%
	3	1,544	75.1%	1,081	71.3%	463	85.7%	1,956	95.1%	1,509	99.5%	447	82.8%
	4	N/A		N/A		N/A		491	95.5%	378	99.7%	113	83.7%
One per RSO	1	39	7.6%	15	4.0%	24	17.8%	56	10.9%	39	10.3%	17	12.6%
	2	423	82.3%	298	78.6%	125	92.6%	503	97.9%	379	100.0%	124	91.9%
	3	475	92.4%	342	90.2%	133	98.5%	507	98.6%	379	100.0%	128	94.8%
	4	N/A		N/A		N/A		491	95.5%	378	99.7%	113	83.7%

problems solved) of each method is shown in Table 1, accounting for all combinations of tracks. Single tracks (i.e.: combinations of one track) and pairs are shown for the sake of completeness and because they might be relevant during track-to-track association. Moreover, a breakdown of the results according to the corresponding RSO eccentricity is also available. Note that the results for combinations of different number of tracks cannot be compared to each other since the total number of combinations varies (e.g.: there are a total of 2,056 combinations of a single track but only 514 of four tracks). To overcome this, we provide also an additional breakdown (*One per RSO*) taking at most one combination per RSO (the best in terms of orbit error).

The number of tracks determines the amount of information available, as well as the observability of the orbit. In fact, only a few combinations and RSOs succeed when only a single track is considered. Gooding's method optimal performance is reached when three tracks are used, since it was conceived for three observations or attributables, while the proposed method is also able to succeed with two and four tracks. Moreover, if considering the whole population (*all* column) Double R-Iteration Lambert leads to higher success rates than Gooding's method. In the case of three tracks, the fairest case for Gooding's method, our method succeed in the 95.1% of the IOD problems (involving the 98.6% of the RSO population), while Gooding's method succeed in the 75.1% of the IOD problems (involving 92.4% of the RSO population). Modest results are obtained with Gooding's method and single tracks and pairs. However, the proposed method is not, in principle, limited to a number of observations or attributables, and, therefore, the number of successes with pairs, triplets and quadruplets is of the same order.

Eccentricity is another driver of IOD performance, as it has a direct impact on orbit observability. To assess the effect of this parameter, the number of successes are broken down in IOD problems involving RSOs with $e < 0.1$ and $e > 0.1$. For low eccentricity RSOs, our method is able to succeed in more than 99% of the IOD problems, involving as well more than 99% of the RSO population, while Gooding's method reaches a 71.3% (90.2% in terms of RSO population) if using three tracks. Regarding RSOs with $e > 0.1$, Gooding's method provide slightly better results in terms of success rates: 85.7% of the IOD problems (98.5% of the RSO population), as opposed to Double R-Iteration Lambert: 82.8% (94.8% of the RSO population), in the case of three tracks.

Nevertheless, the number of successes is just a rough indicator of performance, more focused on robustness as opposed to accuracy. To evaluate the latter, the distributions of the shape and orientation errors of all the combinations for each method are shown in Fig. 8. There is a clear correlation between both errors and a significant difference between the distribution of the Gooding's method solutions and those of the proposed method. As already discussed, the latter is able to succeed in more IOD

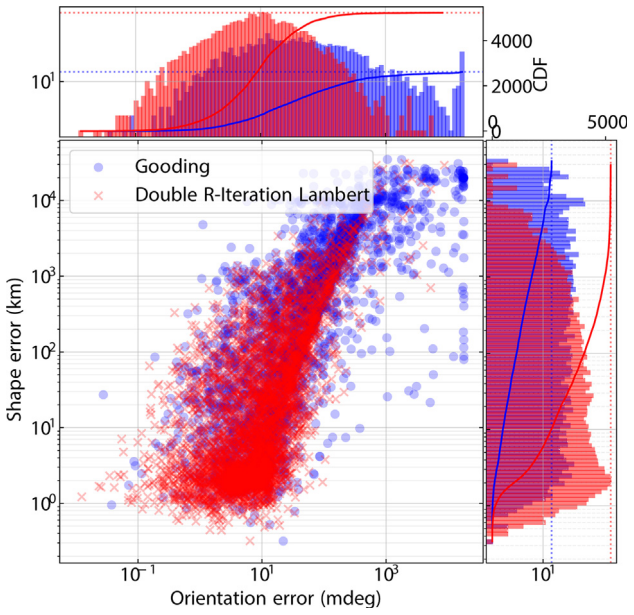

Fig. 8. Distribution of the shape and orientation errors in the optical scenario.

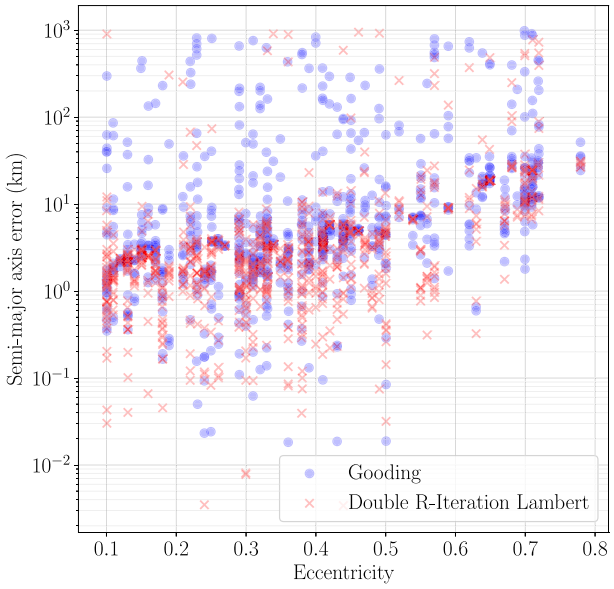

Fig. 9. Distribution of the semi-major axis error along RSO eccentricity in the optical scenario.

problems and therefore its CDF reaches higher values than the former. In terms of the histograms (note the logarithm scale), our method has an error distribution concentrated around values of $d = 2\,\text{km}$ and $\delta = 10\,\text{mdeg}$ and not so spread as that resulting from Gooding's method. The reason of this spread of the error distributions is that Gooding's method is not able to provide reliable results when using two or four tracks, as opposed to the proposed method. However, the range of values swept by the two methods is equivalent, confirming that the accuracy of the two methods is similar, expected since the underlying dynamical model (two-body motion) is the same. This can be seen in Fig. 10 (top) showing the distribution of the semi-major axis error, to ease the physical interpretation, for different number of tracks. The peak, in both cases, is around 2 km (similar to the $\delta = 2\,\text{km}$ observed in Fig. 8) and and the unsuitability of Gooding's method when dealing with two tracks can be observed. The increase of the time of flight with the number of tracks explains the slight differences between the pairs, triplets and quadruplets cases, i.e. there is a trade-off between observation data and dynamical model mismatch. Moreover, a strong

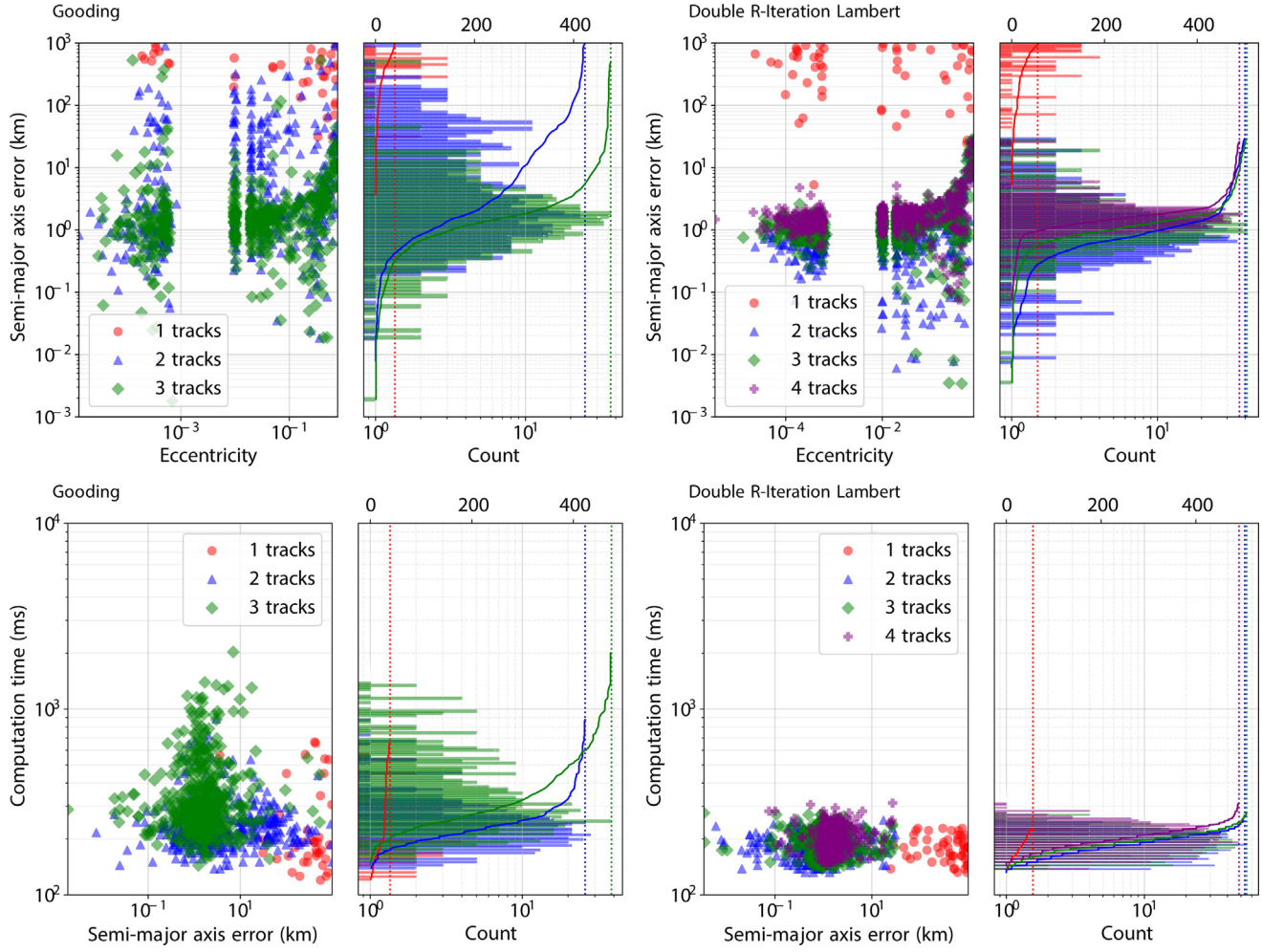

Fig. 10. Distribution of the semi-major axis error and eccentricity in the optical scenario (top) and computational time and semi-major axis error (bottom), one combination per number of tracks and RSO.

increase of the semi-major axis error is noticeable for $e > 0.1$ in both methods. Regardless of the method considered, the higher the eccentricity, the more complex the IOD problem is and therefore the higher the orbital error becomes (see Fig. 9). The two main causes of this are: 1) dynamical behaviour difference between perigee (atmospheric drag) and apogee, and 2) observability issues. Despite of this, the proposed method is able to obtain a first guess of the orbit, that during track-to-track association is refined by incorporating more observations (tracks) and observation geometries (sensors).

Finally, Fig. 10 (bottom) shows the distribution of the computational cost for the two methods, as well as the semi-major axis error distribution. The computational cost of Double R-Iteration Lambert is up to one order of magnitude lower than Gooding's method. This is due to the more direct approach of the former, that avoids finding all the different solutions through iterative processes, as opposed to Gooding's method. In order to compare the distributions of different number of tracks, only the best solution (closer to the true orbit) of each combination of a certain number of tracks and RSO is shown.

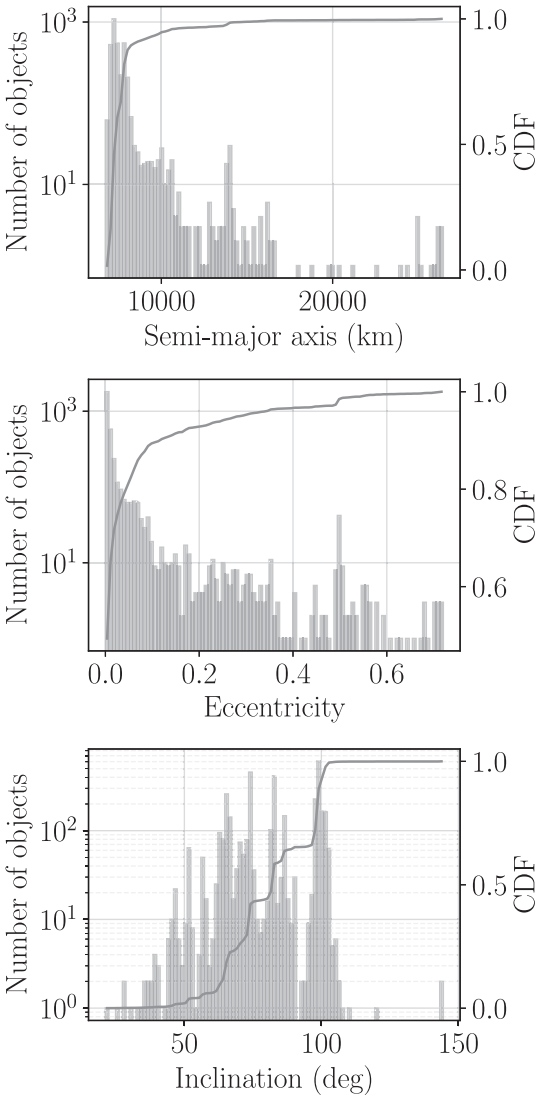

Fig. 11. Semi-major axis (top), eccentricity (center) and inclination (bottom) distribution of the population of RSOs in the radar scenario.

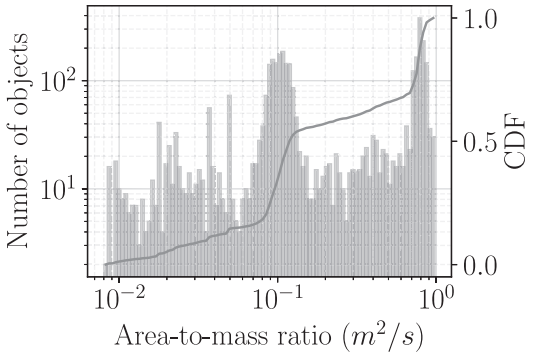

Fig. 12. Area-to-mass ratio distribution of the population of RSOs in the radar scenario.

4.2. Radar observations

The simulated radar scenario consists of 3,664 RSOs and a radar sensor (located in mainland Spain) receiving 14,656 tracks along one week. The semi-major axis, eccentricity and inclination of this population of RSOs and the distribution of the track duration and separation are shown in Fig. 11. The drag coefficient has been set to 2.2 for every object and the area-to-mass ratio distribution of the RSOs is can be seen in Fig. 12. For each RSO, four tracks are generated including zero-mean Gaussian noise of 64.5 mdeg sigma in azimuth and elevation, 3 m in range and 170 mm/s in range-rate, typical values used in similar analyses (Gronchi et al., 2015; Vananti et al., 2017). The duration of the tracks, as shown in Fig. 13 (left), is such that

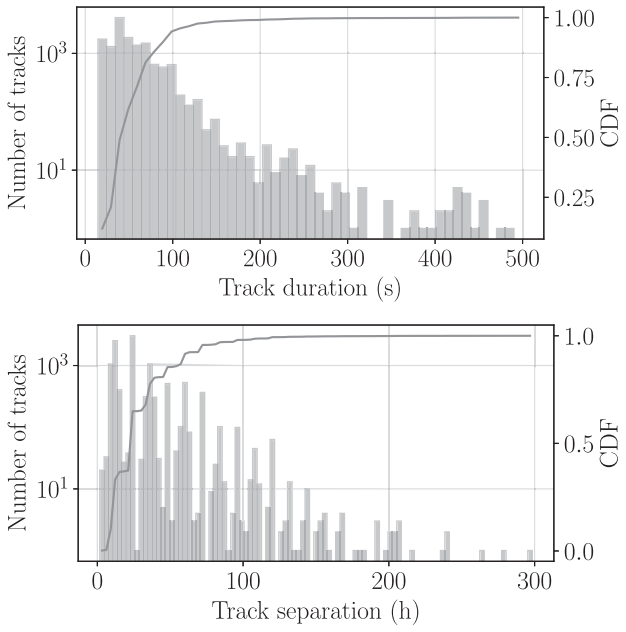

Fig. 13. Track duration (top) and separation (bottom) distributions in the radar scenario.

Table 2
Number of successes and success rate in the radar scenario.

	Number of tracks	Gibbs/Herrick-Gibbs						GTDS Range and Angles						State Vector Fitting					
		all		e<0.1		e>0.1		all		e<0.1		e>0.1		all		e<0.1		e>0.1	
All comb.	1	14,656	100.0%	13,072	100.0%	1,584	100.3%	14,656	100.0%	13,076	100.0%	1,580	100.0%	14,655	100.0%	13,072	100.0%	1,583	100.2%
	2	11,499	52.3%	10,659	54.3%	840	35.4%	N/A		N/A		N/A		21,984	100.0%	19,609	100.0%	2,375	100.2%
	3	3,777	25.8%	3,493	26.7%	284	18.0%	N/A		N/A		N/A		14,648	99.9%	13,068	99.9%	1,580	100.0%
	4	N/A		N/A		N/A		N/A		N/A		N/A		3,649	99.6%	3,254	99.5%	395	100.0%
One per RSO	1	3,664	100.0%	3,269	100.0%	395	100.0%	3,664	100.0%	3,269	100.0%	395	100.0%	3,664	100.0%	3,269	100.0%	395	100.0%
	2	3,189	87.0%	2,951	90.3%	238	60.3%	N/A		N/A		N/A		3,664	100.0%	3,269	100.0%	395	100.0%
	3	1,879	51.3%	1,746	53.4%	133	33.7%	N/A		N/A		N/A		3,664	100.0%	3,269	100.0%	395	100.0%
	4	N/A		N/A		N/A		N/A		N/A		N/A		3,649	99.6%	3,254	99.5%	395	100.0%

90% of the radar tracks have a duration lower than 1.5 min. The separation between each of the four tracks ranges from 2 s up to 5 days, as reflected in Fig. 13 (right). The observation rate is of 0.14 s^{-1} (i.e. one observation every 7.3 s), similar to values used in track-to-track analyses (Vananti et al., 2017). In this case, we focus on the performance of State Vector Fitting and other classical alternatives, Gibbs/Herrick-Gibbs (Gibbs if orbital spacing is above 5 degrees and Herrick-Gibbs otherwise, as suggested in Vallado (1997)) and GTDS Range and Angles.

As in the optical scenario, the number of successes and success rate are shown in Table 2. Unlike the optical scenario, the three methods are able to succeed in most of the single track cases, even those involving RSOs with $e > 0.1$. However, Gibbs/Herrick-Gibbs fails to succeed in almost half of (47.7%) the two tracks cases and most (74.2%) of the three tracks cases, caused by a lack of coplanarity between the involved state vectors, a well known issue (Vallado, 1997) that becomes relevant as the time between observations increases. GTDS Range and Angles method is able to succeed only in single track cases, probably due to the jump introduced by the track separation in the f and g coefficients to be used for the position fitting. Finally, State Vector Fitting is able to succeed in the majority of the cases, even when dealing with more than two tracks.

The distribution of the shape and orientation errors of all the combinations for each method is shown in Fig. 14, where both the histogram and CDF is presented. The CDF of State Vector Fitting is much higher since it is able to succeed with more than one track, unlike the other methods. As in the optical scenario, regardless of the method considered, the higher the eccentricity, the higher the orbital error is (see Fig. 15) since the estimation of eccentric RSOs is much more demanding than circular ones.

The differences between the distributions from the classical methods (Gibbs/Herrick-Gibbs and GTDS Range and Angles) and State Vector Fitting method lie in the fact that the latter includes many IOD problems involving more than one track, which has a negative impact on the orientation error. However, they are very similar on the region that correspond to IOD problems of a single track,

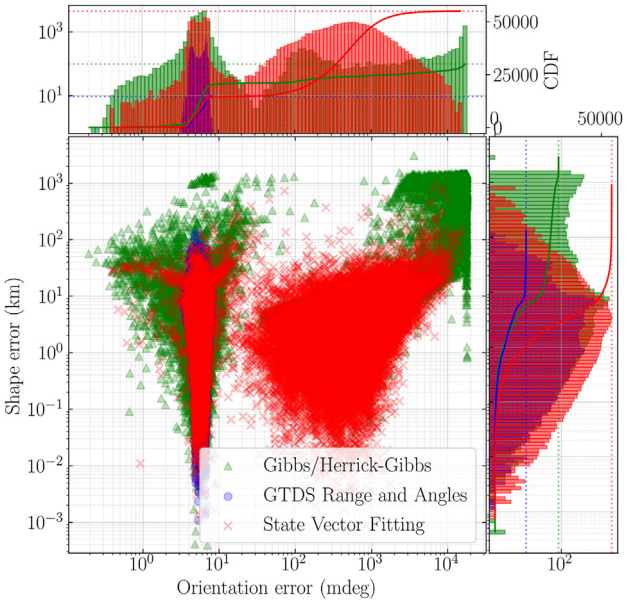

Fig. 14. Distribution of the shape and orientation errors in the radar scenario.

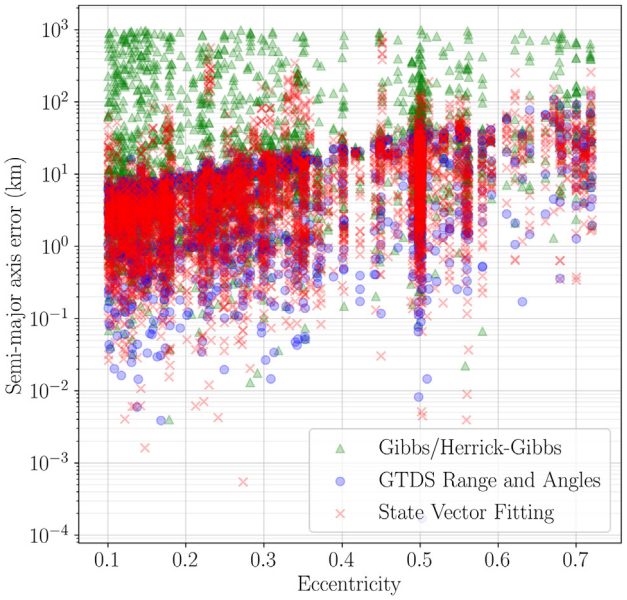

Fig. 15. Distribution of the semi-major axis error along RSO eccentricity in the radar scenario.

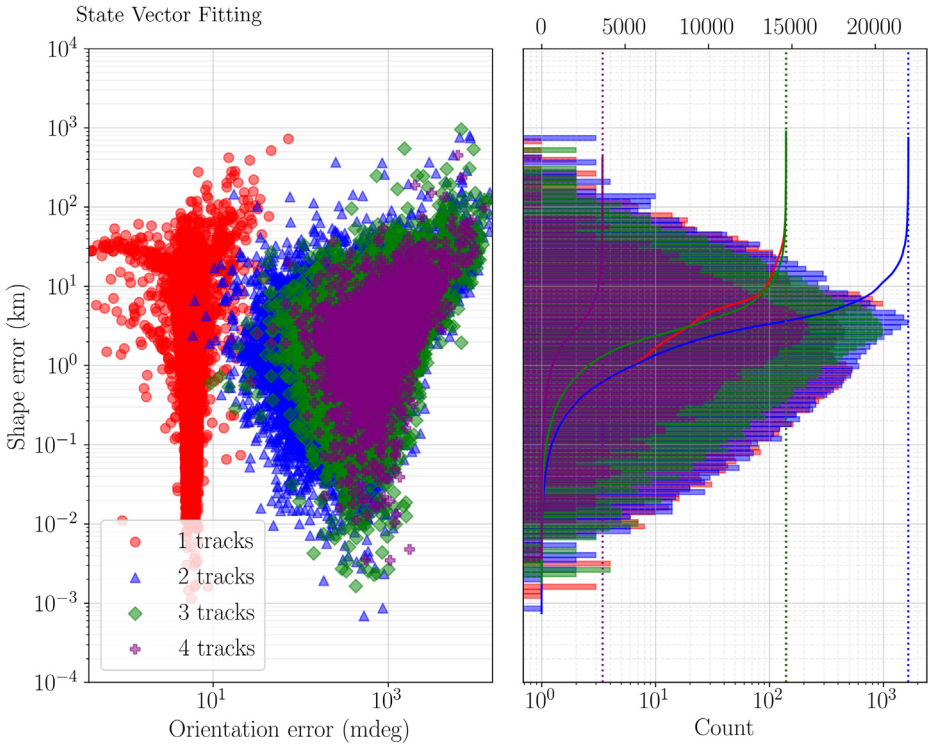

Fig. 16. Distribution of the shape and orientation errors in the radar scenario obtained with State Vector Fitting as a function of the number of tracks.

presenting a peak at $d = 6\,\text{km}$ and $\delta = 5\,\text{mdeg}$. The cluster of points out of this region correspond to cases of two and more tracks, and it is mainly populated by State Vector Fitting solutions, as discussed before. These IOD solutions have similar shape errors as the single track ones, but an orientation error that increases with the number of tracks (see Fig. 16). Although this might appear unexpected at first sight, it is related to the track separation and the effect of the lack of atmospheric drag modelling. In the single track case, only one state vector is computed, but in the case of i tracks, i equinoctial elements state vectors are computed and averaged, which implies that the fast variable should be propagated before averaging. Since the equivalent dynamical model of this propagation is the two-body motion, the atmospheric drag effect is accumulated on the estimation of the fast variable.

Fig. 17 shows the distribution of the computational cost for the two methods. The apparent lack of continuity is caused by the computational time tracker, limited by a minimum step. The first noticeable difference with respect to the optical cases is the order or magnitude of the computational time, up to one order of magnitude greater than Gooding's method. Apart from that, there are no major differences between the three methods.

5. Conclusions

This paper has presented two IOD methods proposed for optical and radar track-to-track association. Double r-iteration Lambert is a novel method that formulates the angles-only IOD problem as a boundary value problem in which a pair of ranges is estimated so that the residuals

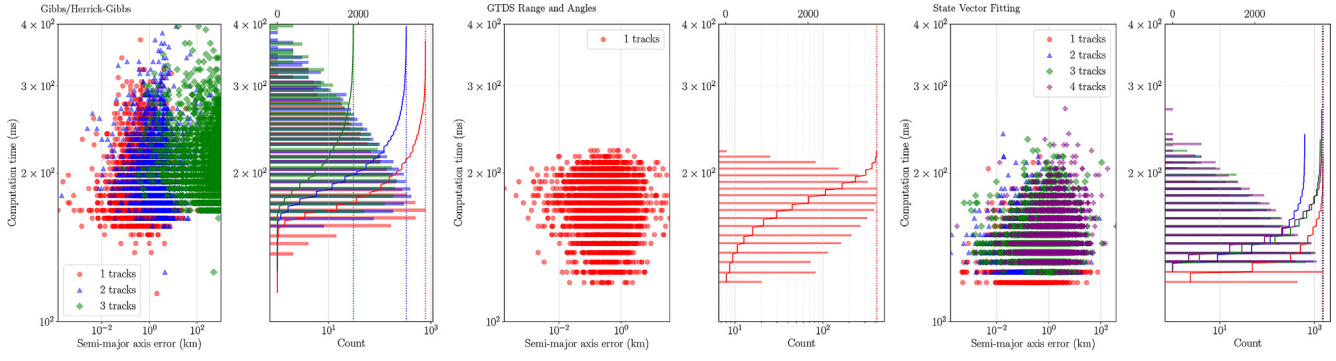

Fig. 17. Distribution of the computational time and semi-major axis error in the radar scenario, one combination per number of tracks and RSO.

Table 3
IOD methods analysed.

	Method	Tracks	Obs.
Optical	Gooding	2 or 3	3
	Double R-Iteration Lambert	**> 1**	**> 2**
Radar	Gibbs/Herrick-Gibbs	1, 2 or 3	3
	GTDS Range and Angles	1	>1
	State Vector Fitting	**Any**	**> 1**

of the available observations are minimised. It allows to consider measurement noise and provides a full estimation (i.e., state vector and covariance). Additionally, State Vector Fitting is a method that fits the states observed by radar sensors to obtain a smooth solution, thus mitigating measurement noise. The two methods are able to use an arbitrary number of observations and do not require prior information nor are limited to circular orbits. Moreover, they have been shown to be more robust (according to the metric defined) and less computationally intensive, while providing similar orbital errors than classical alternatives, such as Gooding, Gibbs/Herrick-Gibbs and GTDS Range and Angles methods. All the methods considered are summarised in Table 3, with the proposed ones in bold font, shown to be more suitable for track association purposes.

This work fills the gaps between IOD and track association during cataloguing of RSOs by describing methods for radar and optical observations. We have also given a hint on the relevance of track association, particularly during catalogue build-up, i.e.: before performing the first estimation of an RSO orbit, and optical tracks. In fact, it is clear that in this case, some form of brute-force would be required, since a single optical track might not be sufficient for an IOD.

Declaration of Competing Interest

The authors declare that they have no known competing financial interests or personal relationships that could have appeared to influence the work reported in this paper.

Acknowledgments

This project has received funding from the "Comunidad de Madrid" under "Ayudas destinadas a la realización de doctorados industriales" program (project IND2017/TIC7700). Besides, the authors would like to acknowledge the contributions from Alfredo Miguel Antón Sácnchez, Pablo García Sánchez and Adrián Díez Martín from GMV for their support, review and advice.

References

18th Space Control Squadron, 2020. Space-track. https://www.space-track.org [Online; accessed 12-February-2020].

Alarcón, J.R., Klinkrad, H., Cuesta, J., Martinez, F.M., 2005. Independent orbit determination for collision avoidance. In: D. Danesy (Ed.), 4th European Conference on Space Debris. volume 587 of ESA Special Publication. p. 331. http://adsabs.harvard.edu/abs/2005ESASP.587.331A.

Aristoff, J.M., Horwood, J.T., Singh, N., Poore, A.B., Sheaff, C., Jah, M. K., 2013. Multiple Hypothesis Tracking (MHT) for space surveillance: theoretical framework. In: AAS/AIAA Astrodynamics Specialist Conference.

Armellin, R., Lizia, P.D., 2016. Probabilistic optical and radar initial orbit determination. In: AAS/AIAA Astrodynamics Specialist Conference, vol. 41. American Institute of Aeronautics and Astronautics (AIAA), pp. 101–118. https://doi.org/10.2514/1.g002217.

Armellin, R., Lizia, P.D., Zanetti, R., 2016. Dealing with uncertainties in angles-only initial orbit determination. Celestial Mech. Dyn. Astronomy 125, 435–450. https://doi.org/10.1007/s10569-016-9694-z.

Fontdecaba i Baig, J., Martinerie, F., Sutter, M., Martinot, V., Fletcher, E., 2011. Radar tracking campaigns for ESA CO-VI. In: European Space Surveillance Conference.

Bar-Shalom, Y., 1981. On the track-to-track correlation problem. IEEE Trans. Autom. Control 26, 571–572. https://doi.org/10.1109/tac.1981.1102635.

Bar-Shalom, Y., Li, X.-R., Kirubarajan, T., 2001. Estimation with Applications to Tracking and Navigation. John Wiley & Sons Inc.. https://doi.org/10.1002/0471221279.

Bennett, J., Sang, J., Smith, C., Zhang, K., 2012. Improving low-earth orbit predictions using two-line element data with bias correction. In: Advanced Maui Optical and Space Surveillance Technologies Conference, p. 46.

Blackman, S.S., 2004. Multiple hypothesis tracking for multiple target tracking. IEEE Aerosp. Electron. Syst. Mag. 19, 5–18. https://doi.org/10.1109/maes.2004.1263228.

Broucke, R.A., Cefola, P.J., 1972. On the equinoctial orbit elements. Celestial Mech. 5, 303–310. https://doi.org/10.1007/bf01228432.

Cefola, P.J., 2012. Fortran 77 DSST standalone orbit propagator design document. Technical Report University at Buffalo.

DeMars, K.J., Jah, M.K., 2013. Probabilistic initial orbit determination using gaussian mixture models. J. Guidance, Control, Dyn. 36, 1324–1335. https://doi.org/10.2514/1.59844.

DeMars, K.J., Jah, M.K., Schumacher, P.W., 2012. Initial orbit determination using short-arc angle and angle rate data. IEEE Trans. Aerosp. Electron. Syst. 48, 2628–2637.

Dhar Sha, K., Dash, D., 2017. A probabilistic multiple hypothesis tracking system for space object tracking. International Journal of Innovative Science. Eng. Technol.

Domínguez-González, R., Sánchez-Ortiz, N., Guijarro-López, N., Quiles-Ibernón, P., Nomen-Torres, J., 2017. Cataloguing space objects from observations: Corto cataloguing system. In: 7th European Conference on Space Debris.

Eckstein, M., Hechler, F., 1970. A reliable derivation of the perturbations due to any zonal and tesseral harmonics of the geopotential for nearly-circular satellite orbits. Technical Report ESA, Darmstadt, Germany. ESRO SR-13-1970.

Escobal, P., 1965. Methods of Orbit Determination, 2nd ed. Krieger Publishing, Robert E.

Fujimoto, K., Scheeres, D.J., Herzog, J., Schildknecht, T., 2013. Association of short-arc optical tracks via the direct bayesian admissible region: theory and application. In: 6th European Conference on Space Debris.

Galbreath, E.A., 1970. Brouwer-Lyddane orbit generator routine. Technical Report NASA. Goddard Space Flight Center.

Gauss, C.F., 1809. Theoria Motus Corporum Coelestium in Sectionibus Conicis Solem Ambientium. Cambridge Library Collection - Mathematics. Cambridge University Press. https://doi.org/10.1017/CBO9780511841705.

Gooding, R., 1990. A procedure for the solution of lambert's orbital boundary-value problem. Celestial Mech. Dyn. Astron. 48, 145–165. https://doi.org/10.1007/BF00049511.

Gooding, R., 1993. A New Procedure for Orbit Determination Based on Three Lines of Sight (Angles Only). Technical Report Defence Research Agency.

Gronchi, G.F., Baù, G., Milani, A., 2016. Keplerian integrals, elimination theory and identification of very short arcs in a large database of optical observations. Celestial Mech. Dyn. Astron. 127, 211–232. https://doi.org/10.1007/s10569-016-9725-9.

Gronchi, G.F., Dimare, L., Cioci, D.B., Ma, H., 2015. On the computation of preliminary orbits for earth satellites with radar observations. Mon. Not. R. Astron. Soc. 451, 1883–1891. https://doi.org/10.1093/mnras/stv1010.

Haimerl, J., Fonder, G., 2015. Space fence system overview. In: Proceedings of the Advanced Maui Optical and Space Surveillance Technology Conference. Curran Associates, Inc., Redhook, NY.

Herzog, J., Schildknecht, T., Hinze, A., 2013. Space surveillance observations at the AIUB Zimmerwald observatory. In: 6th European Conference on Space Debris Conference.

Hill, K., Alfriend, K., Sabol, C., 2008. Covariance-based uncorrelated track association. In: AIAA/AAS Astrodynamics Specialist Conference and Exhibit. American Institute of Aeronautics and Astronautics. https://doi.org/10.2514/6.2008-7211.

Hill, K., Sabol, C., Alfriend, K.T., 2012. Comparison of covariance based track association approaches using simulated radar data. J. Astronaut. Sci. 59, 281–300. https://doi.org/10.1007/s40295-013-0018-1.

Hussein, I.I., Roscoe, C.W.T., Wilkins, M.P., Schumacher, P.W., 2015. On mutual information for observation-to-observation association. In: 2015 18th International Conference on Information Fusion (Fusion), pp. 1293–1298.

Hussein, I.I., Roscoe, C.W.T., Wilkins, M.P., Schumacher Jr., P.W., 2015. Track-to-track association using bhattacharyya divergence. In: Advanced Maui Optical and Space Surveillance Technologies (AMOS) Conference.

Izzo, D., 2014. Revisiting Lambert's problem. Celestial Mech. Dyn. Astron. 121, 1–15. https://doi.org/10.1007/s10569-014-9587-y.

Johns, L., Shaw, A., Ray, A., 1990. Orbiting debris: a space environmental problem. Technical Report OTA-BP-ISC-72 Office of Technological Assessment.

Jones, B.J., Vo, B.-N., 2015. A labeled multi-bernoulli filter for space object tracking. In: AAS/AIAA Astrodynamics Specialist Conference.

Jordan, J.F., 1964. The Application of Lambert's Theorem to the Solution of Interplanetary Transfer Problems. Technical Report Jet Propulsion Laboratory, California Institude of Technology.

JSC Vimpel Interstate Corporation and the Keldysh Institute of Applied Mathematics, JSC Vimpel data portal, 2020. http://spacedata.vimpel.ru/ [Online; accessed 12-February-2020].

Kelso, T., 2020. Celestrack SATCAT. https://celestrak.com [Online; accessed 30-November-2020].

Laplace, P.-S., 1780. Mémoire sur la détermination des orbites des comètes volume 10. In: Mémoires de l'Académie royale des sciences de Paris.

Long, A., Cappellari, J., Velez, C., Fuchs, A., 1989. Goddard Trajectory Determination System (GTDS) - Mathematical Theory - Revision 1. Technical Report FDD/552-89/001 and CSC/TR-89/6001 National Aeronautics and Space Administration and Computer Sciences Corporation.

Marquardt, D.W., 1963. An algorithm for least-squares estimation of nonlinear parameters. J. Soc. Ind. Appl. Math. 11, 431–441. https://doi.org/10.1137/0111030.

Martinez Fadrique, F., Águeda Maté, A., Jorquera Grau, J., Fernández Sánchez, J., Aivar García, L., 2011. Comparison of angles only initial orbit determination algorithms. In: 22nd International Symposium on Space Flight Dynamics.

Milani, A., Gronchi, G.F., Vitturi, M.D.M., Kneževic, Z., 2004. Orbit determination with very short arcs. I admissible regions. Celestial Mech. Dyn. Astron. 90, 57–85. https://doi.org/10.1007/s10569-004-6593-5.

Milani, A., Sansaturio, M., Chesley, S., 2001. The asteroid identification problem IV: Attributions. Icarus 151, 150–159. https://doi.org/10.1006/icar.2001.6594.

Montenbruck, O., Gill, E., 2000. Satellite Orbits: Models, Methods and Applications. Springer-Verlag, Berlin Heidelberg. https://doi.org/10.1007/978-3-642-58351-3.

Mortari, D., Scuro, S.R., Bruccoleri, C., 2006. Attitude and orbit error in n-dimensional spaces. J. Astronaut. Sci. 54, 467–484. https://doi.org/10.1007/bf03256501.

Morton, B.G., Taff, L.G., 1986. A new method of initial orbit determination. Celestial Mech. 39, 181–190. https://doi.org/10.1007/bf01230850.

Olmedo, E., Sánchez-Ortiz, N., Lerate, M.R., Belló-Mora, M., Klinkrad, H., Pina, F., 2008. Initial orbit determination algorithms for cataloguing optical measurements of space debris. Mon. Not. R. Astron. Soc. 391, 1259–1272. https://doi.org/10.1111/j.1365-2966.2008.13940.x.

Pastor, A., Escobar, D., Sanjurjo-Rivo, M., Águeda, A., 2018. Object detection methods for radar survey measurements. In: 69th International Astronautical Congress. https://iafastro.directory/iac/paper/id/44403/summary/iAC-18, A6,9,9, x44403.

Pastor, A., Escobar, D., Sanjurjo-Rivo, M., Águeda, A., 2019. Object detection methods for optical survey measurements. In: 20th Advanced Maui Optical and Space Surveillance Technologies.

Pirovano, L., Principe, G., Armellin, R., 2020. Data association and uncertainty pruning for tracks determined on short arcs. Celestial Mech. Dyn. Astron. 132. https://doi.org/10.1007/s10569-019-9947-8.

Poore, A.B., Aristoff, J.M., Horwood, J.T., Armellin, R., Cerven, W.T., Cheng, Y., Cox, C.M., Erwin, R.S., Frisbee, J.H., Hejduk, M.D., Jones, B.A., Di Lizia, P., Scheeres, D.J., Vallado, D.A., Weisman, R. M., 2016. Covariance and Uncertainty Realism in Space Surveillance and Tracking. Technical Report Numerica Corporation Fort Collins United States. URL https://apps.dtic.mil/docs/citations/AD1020892.

Pulford, G., 2005. Taxonomy of multiple target tracking methods. IEE Proceedings-Radar, Sonar Navigat. 152, 291–304.

Rodriguez Fernandez, O., Utzmann, J., Bonaventure, F., Gegout, D., Nicolls, M., Griffith, N., 2018. Evaluation of a commercial radar network to support conjunction assessment. In: 69th International Astronautical Congress (IAC), IAC-18-A6.7.4.x44472..

Sabol, C., Schumacher, P., Segerman, A., Coffey, S., Hoskins, A., 2012. Search and Determine Integrated Environment (SADIE). In: Advanced Maui Optical and Space Surveillance Technologies (AMOS) Conference, p. 54.

Schildknecht, T., 2007. Optical surveys for space debris. Astron. Astrophys. Rev. 14, 41–111. https://doi.org/10.1007/s00159-006-0003-9.

Schildknecht, T.e.a., 2005. Properties of the high area-to-mass ratio space debris population in GEO. In: Advanced Maui Optical and Space Surveillance Technologies (AMOS) Conference.

Siminski, J., 2016. Techniques for assessing space object cataloguing performance during design of surveillance systems. In: 6th International Conference on Astrodynamics Tools and Techniques (ICATT). 14-17 March 2016, Darmstadtium.

Siminski, J., Montenbruck, O., Fiedler, H., Schildknecht, T., 2014. Short-arc tracklet association for geostationary objects. Adv. Space Res. 53, 1184–1194. https://doi.org/10.1016/j.asr.2014.01.017.

Singh, N., Poore, A., Sheaff, C., Aristoff, J., Jah, M., 2013. Multiple Hypothesis Tracking (MHT) for space surveillance: results and simulation studies. In: Advanced Maui Optical and Space Surveillance Technologies (AMOS) Conference, p. E16.

Springer, T.A., 2009. NAPEOS Mathematical Models and Algorithms. Technical Report European Space Agency.

Stauch, J., Bessell, T., Rutten, M., Baldwin, J., Jah, M., Hill, K., 2018. Joint probabilistic data association and smoothing applied to multiple space object tracking. J. Guidance, Control, Dyn. 41, 19–33. https://doi.org/10.2514/1.g002230.

Tapley, B.D., Schutz, B.E., Born, G.H., 2004. Statistical Orbit Determination. Elsevier Academic Press.

Tommei, G., Milani, A., Rossi, A., 2007. Orbit determination of space debris: admissible regions. Celestial Mech. Dyn. Astron. 97, 289–304.

Uhlmann, J.K., 2008. Introduction to the algorithms of data association in multiple-target tracking. In: Liggins, M.E., Hal, D.L., Llinas, J. (Eds.), Handbook of Multisensor Data Fusion: Theory and Practice chapter 4, 2nd ed. CRC Press.

Vallado, D., Crawford, P., Hujsak, R., Kelso, T.S., 2006. Revisiting spacetrack report #3: Rev 2. In: AIAA/AAS Astrodynamics Specialist

Conference and Exhibit. American Institute of Aeronautics and Astronautics. https://doi.org/10.2514/6.2006-6753.

Vallado, D.A., 1997. Fundamentals of Astrodynamics and Applications. Springer-Verlag, New York.

Vananti, A., Schildknecht, T., Siminski, J., Flohrer, T., Jilete, B., 2016. Association of tracklets from angular and range measurements. In: Final Stardust Conference. 31st Oct – 4th Nov 2016, ESA ESTEC, The Netherlands.

Vananti, A., Schildknecht, T., Siminski, J., Jilete, B., Flohrer, T., 2017. Tracklet-tracklet correlation method for radar and angle observations. In: 7th European Conference on Space Debris. Darmstadt, Germany. 18 - 21 April 2017.

Warner, J.G., Lemm, K., 2016. Comparing radius of convergence in solving the nonlinear least squares problem for precision orbit determination of geodetic satellites. In: AIAA/AAS Astrodynamics Specialist Conference. American Institute of Aeronautics and Astronautics. https://doi.org/10.2514/6.2016-5339.

Weisman, R.M., Jah, M.K., 2014. Uncertainty quantification for angles-only initial orbit determination. In: AAS/AIAA Space Flight Mechanics Conference.

Yanez, C., Dolado, J.C., Richard, P., Lllamas, I., Lapasset, L., 2017. Optical measurements association using optimized boundary value initial orbit determination coupled with markov clustering algorithm. J. British Interplanet. Soc. 70, 69–76.

Yanez, C., Mercier, F., Dolado, J.C., 2017. A novel initial orbit determination algorithm from doppler and angular observations. In: 7th European Conference on Space Debris.

Zeinalov, R., 1973. Determination of a circular orbit for an earth satellite from optical observations at unknown times. Soviet Astron. 17, 131.